

1     **High-resolution in vivo fundus angiography without the need for an**  
2                                   **adaptive optics imaging system**

3  
4     Mali Okada, MMed<sup>1,2</sup>; Tjebo FC Heeren, MD<sup>2,3</sup>; Pádraig J Mulholland, PhD<sup>2,3,4</sup>; Peter M  
5             Maloca, MD<sup>2,5-7</sup>; Marketa Cilkova, MSc<sup>3</sup>; Vincent Rocco<sup>2</sup>; Marcus Fruttiger PhD<sup>3</sup>;  
6             Catherine A Egan, FRANZCO<sup>2,3</sup>; Roger S Anderson, DSc<sup>2,3,4</sup>; Adnan Tufail, MD  
7                                   FRCOphth<sup>2,3</sup>

- 8  
9     1. Royal Victorian Eye and Ear Hospital, Melbourne Australia  
10    2. Moorfields Eye Hospital NHS Foundation Trust, London, United Kingdom  
11    3. Institute of Ophthalmology, University College London, London, United Kingdom  
12    4. Optometry and Vision Sciences Research Group, School of Biomedical Science,  
13        Ulster University, Coleraine, Northern Ireland  
14    5. OCTlab, Department of Ophthalmology, University Hospital Basel, Basel,  
15        Switzerland  
16    6. Institute of Molecular and Clinical Ophthalmology Basel (IOB), Basel, Switzerland  
17    7. Department of Ophthalmology, University of Basel, Basel, Switzerland

18  
19  
20

21    **Short title:** High resolution fundus angiography

22

23    **Financial disclosures:** MO – Allergan; Bayer RSA, PJM – Heidelberg Engineering; AT -  
24    Novartis, Roche, Allergan, Alcon, Heidelberg Engineering

25

26    **Funding:** AT and CE are funded by the United Kingdom's National Institute for Health  
27    Research of Health's Biomedical Research Centre for Ophthalmology at Moorfields Eye  
28    Hospital and UCL Institute of Ophthalmology. The views expressed are those of the authors,  
29    not necessarily those of the Department of Health. The funder had no role in study design,  
30    data collection, analysis, or interpretation, or the writing of the report.

31

1 **Acknowledgements:** Yoshihika Katayama and Heidelberg engineering for their technical  
2 expertise with the HRA device

3

4 **Address for correspondence:**

5 Adnan Tufail, MD, FRCOphth

6 Moorfields Eye Hospital NHS Trust

7 162 City Road, London, United Kingdom

8 E-mail: Adnan.Tufail@moorfields.nhs.uk

9

10

11

12

1 **Abstract**

2

3 **Purpose:**

4 To provide a proof of concept for the detailed characterization of retinal capillary  
5 features and surrounding photoreceptor mosaic using a customized non-adaptive  
6 optics angiography imaging system.

7

8 **Methods:**

9 High-resolution fluorescein angiography (FFA) and/or indocyanine green  
10 angiography (ICGA) images were obtained using a modified Heidelberg Retina  
11 Angiograph (HRA2) device with a reduced scan angle enabling 3° field of view. Co-  
12 localized images of the photoreceptor mosaic were also captured *in vivo* using the  
13 same instrument. Visibility of vascular sub-branches were compared between high-  
14 resolution images and conventional fundus angiography (FA) with a 30° field of  
15 view.

16

17 **Results:**

18 High-resolution angiographic and infrared images (3° x 3° field of view, a 10-fold  
19 magnification) were obtained in ten participants. These included seven patients with  
20 various retinal diseases, including myopic degeneration, diabetic retinopathy, macular  
21 telangiectasia and central serous chorioretinopathy, as well as three healthy controls.  
22 Images of the retinal vasculature down to the capillary level were obtained on  
23 angiography with the ability to visualize a mean 1.2 levels more sub-branches as  
24 compared to conventional FA. In addition, imaging of the photoreceptor cone mosaic,  
25 to a sufficient resolution to calculate cone density, was possible. Movement of blood  
26 cells within the vasculature was also discernible on infrared videography.

27

28 **Conclusion:**

29 This exploratory study demonstrates that fast high-resolution angiography and cone  
30 visualization is feasible using a commercially available imaging system.

31

32 **Translational Relevance:**

33 This offers potential to better understand the relationship between the retinal neuro-  
34 vascular system in health and disease and the timing of therapeutic interventions in  
35 disease states.

1

2 **Word Count: 247**

## 1 **Introduction**

2

3 Fundus fluorescein angiography (FFA) was first described by Novotny and Alvis in  
4 1961 and has since become the gold standard imaging technique for assessing  
5 macular and retinovascular disorders.<sup>1</sup> Along with indocyanine green angiography  
6 (ICGA) for examining the choroidal circulation, FFA has been instrumental in  
7 developing our understanding of the pathogenesis of many retinal and choroidal  
8 diseases. However, fundus angiography (FA) in its current form has several  
9 limitations. Although recent advances have been made with ultra-wide field  
10 angiography, the resolution of FA remains a limiting factor for studying microscopic  
11 features of the retinal vasculature and the associated neuroretina.

12

13 In the search for accessible higher resolution retinal imaging, optical coherence  
14 tomography angiography (OCTA) is an emerging imaging modality that has been  
15 proposed as an alternative to FA for mapping retinal vessels. It is non-invasive and  
16 provides detailed delineation of the retinal capillary beds. However, it is subject to  
17 projection and motion artefacts and the current technology is unable to demonstrate  
18 flow or leakage.<sup>2</sup> In addition, although OCTA provides some structural information  
19 about the neuroretina, this is not at the cellular level (e.g. photoreceptor mosaics).

20

21 Adaptive optics (AO) based imaging system is another approach that has  
22 demonstrated great potential for imaging the retinal vasculature down to the capillary  
23 level.<sup>3,4</sup> This method has been widely used to investigate the neuroretinal structure,  
24 principally cone photoreceptor mosaics<sup>3-5</sup>. Two methods of adaptive optics scanning  
25 light ophthalmoscopy (AOSLO) system have been employed to image retinal vessels,  
26 including a confocal system combined with oral fluorescein, as well as a non-confocal  
27 AOSLO system, which is coupled with motion contrast to remove the need for  
28 contrast agents.<sup>6-8</sup>

29

30 Although these AO based imaging systems provide unparalleled resolution of the  
31 retinal microstructure, they are complex, expensive, require significant patient  
32 cooperation and image processing. As such, it is currently impractical to use in  
33 routine clinical practice or in large-scale clinical trials. A simpler, non-AO based  
34 system that can resolve images *in vivo* down to the level of photoreceptors and small  
35 retinal capillaries, has the potential to provide novel insights into retinal disease and

1 may provide endpoints for future clinical studies. The ability to image larger numbers  
2 of patients with various levels of disease than is currently feasible using current AO  
3 systems would also help to generate new biomarkers in our understanding of  
4 retinovascular diseases. Although we have previously demonstrated that the  
5 paramacular cone mosaic may be imaged in vivo using a modified scanning laser  
6 ophthalmoscope,<sup>9,10</sup> the capabilities of the device to provide high resolution  
7 angiography has not been examined. Therefore, the aim of this exploratory study is to  
8 provide a proof-of-concept demonstration of high-resolution angiography alongside  
9 photoreceptor imaging using a modified commercially available non-adaptive optics  
10 imaging device.

11

## 12 **Methods**

13

### 14 *Participants*

15 Participants for this exploratory study were recruited from the medical retina clinics at  
16 Moorfields Eye Hospital. They were invited to join the study if they had retinal  
17 pathology requiring FFA and/or ICGA diagnostic workup as part of their clinical care.  
18 Additional healthy control participants were also recruited for comparative purposes.  
19 Participants were excluded if they had an allergy to intravenous dye, were aged less  
20 than 18 years, or had significant media pathology that would preclude good quality  
21 imaging on conventional FA.

22

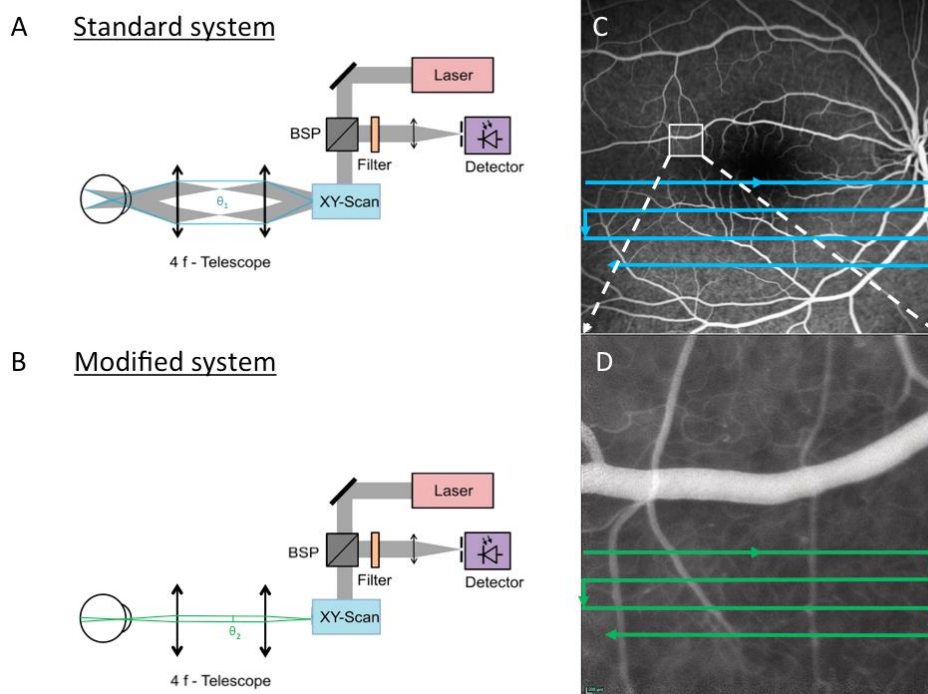
23 Ethics approval was obtained approved by the local institutional review board and  
24 conducted according to the tenets of the Declaration of Helsinki. Written informed  
25 consent was obtained from all participants.

26

### 27 *High-resolution Fundus Angiography*

28 High-resolution imaging was performed using a modified Heidelberg Retina  
29 Angiograph 2 (HRA2; Heidelberg Engineering GmbH, Heidelberg, Germany). This  
30 modification has been previously described for use in cone imaging by our team.<sup>9</sup> In  
31 summary, the standard scan angle of a conventional HRA2 was reduced by a factor of  
32 x10, from 30° field of view down to 3°, with the narrow angle enabling a  
33 magnification of the image whilst retaining the same 768 x 768 density of pixels  
34 (Figure 1). The field of imaging was 3° x 3°, which corresponds to an area on the  
35 retina of 0.825 x 0.825 mm, when calculated using standardized conversion rates at

1 equivalent retinal loci.<sup>11</sup> The original commercial filters for FFA and ICG in the  
 2 HRA2 were left in situ. The incident beam power however of the blue laser (488 nm)  
 3 used for FFA and for blue reflectance imaging was reduced to 100 $\mu$ W to meet the  
 4 requirements for Class 1 emission limit according to the International Electrotechnical  
 5 Commission 60825-1 guidelines. The high-resolution ICGA was acquired with the  
 6 standard diode laser emitting 785 nm, with no change to laser output needed to meet  
 7 safety guidelines. Cone imaging of the same location was also obtained using the  
 8 infrared laser but with the image acquisition set to reflectance mode. Near infrared  
 9 autofluorescence (IRAF) was also performed in some patients to attempt to image the  
 10 retinal pigment epithelium and choriocapillaris layer.  
 11



12  
 13 Figure 1. Schematic of (A) conventional Heidelberg HRA2 device with standard scanning angle ( $\theta_1$ )  
 14 and (B) modified high-resolution device with reduced scan angle ( $\theta_2$ ). (C) High resolution image with a  
 15 scan angle of 3° superimposed onto conventional image of 30°  
 16

17

### 18 *Imaging Protocol*

19 *In vivo* imaging was performed through dilated pupils with different areas of the  
 20 fundus imaged by adjustment of the internal fixation lights. Standard doses of either  
 21 2-3 mls of 20% sodium fluorescein dye or 25mg/5ml of indocyanine green dye were  
 22 injected for FFA and ICGA respectively. Based on the clinical indication for the  
 23 conventional FA, the majority of participants had early phase angiography images

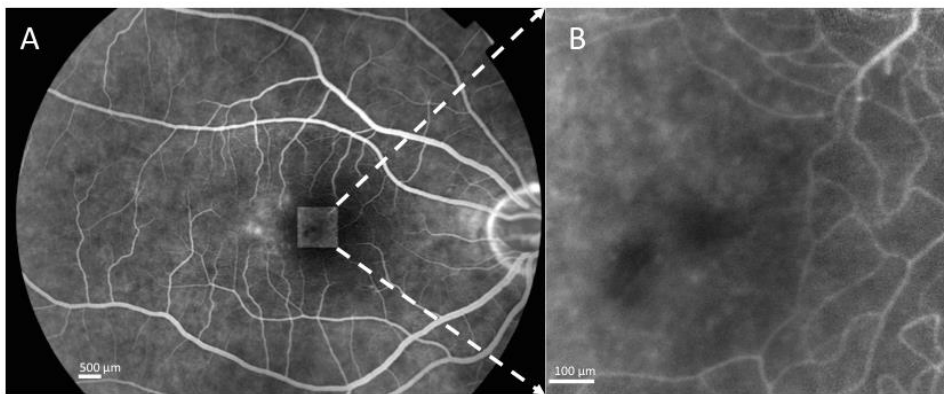
1 conducted on a conventional non-modified HRA2 device with late phase images (> 5  
2 minutes) on the high-resolution device. This was done in order to have both  
3 conventional and high resolution FA performed in the same sitting. In one participant,  
4 imaging was performed on three FA devices to enable comparisons across different  
5 imaging platforms: conventional HRA2, high-resolution HRA2 and Topcon TRC-  
6 NW8 retinal camera (Topcon Medical Systems Inc., USA). In each participant, the  
7 device was then switched to infrared reflectance mode to capture the cone mosaic  
8 pattern at the same location as the FA imaging. Single, non-averaged images as well  
9 as averaged real time (ART) images of 10-40 frames were acquired for both  
10 conventional and high-resolution images. Videography was also obtained to record  
11 blood flow.

12

13 *Image Analysis*

14 Raw images were exported from Heidelberg Eye Explorer with the image borders  
15 cropped to remove other features (eg. date information, patient-identifying data). The  
16 high-resolution images, comprising a 3° x 3° field (768 x 768 pixels), were exported  
17 into Adobe Photoshop CS 5.1 (Adobe Systems Inc, California, USA) and scaled to  
18 size to enable manual overlay onto the corresponding conventional image for  
19 localization and comparison (Figure 2).

20



21

22 Figure 2. Localization and scaling of conventional image (A) and high-resolution image (B)

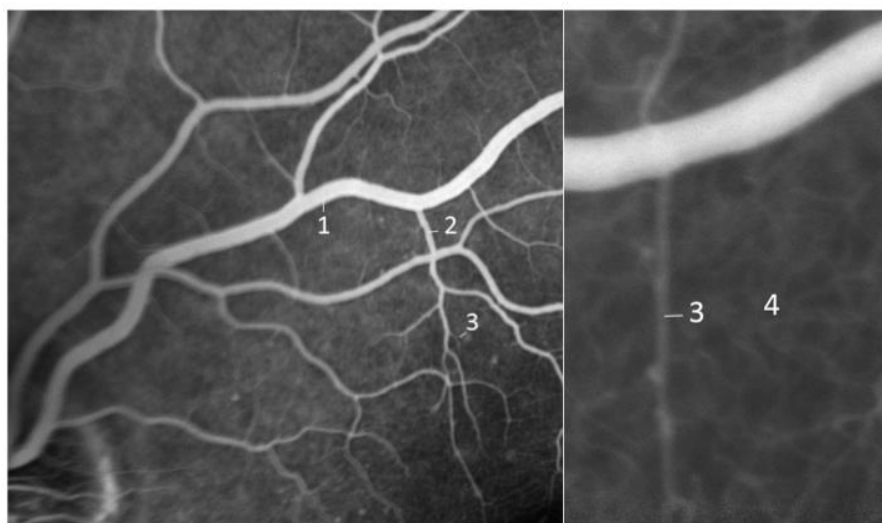
23

24

25 Comparison between conventional and high-resolution images was made for each  
26 patient on a qualitative basis on the clarity of large vessels and quantitatively by the  
27 visibility of sub-branches off the main retinal vascular arcade at the same location  
28 with hierarchical numbering from branch 1 indicating main retinal arcade and 4  
29 indicating capillary network (Figure 3). The difference between the two was



1 calculated with a higher number indicating a step further in the hierarchy of vascular  
2 branching. Analysis of cone density was performed using Matlab software (R2014b,  
3 Mathworks Inc.), according to the automated method described by Li and Roorda for  
4 use in AO images.<sup>12</sup> In brief, image labels were cropped from the raw image and a  
5 low-pass filter then applied. The image was then converted back to the spatial domain  
6 and maximum local luminance was detected and plotted as cone centers, ensuring that  
7 identified cones were not closer than physiologically possible. Manual calculation  
8 was also performed to account for cones erroneously detected over any large blood  
9 vessels. Voronoi analysis was used to examine the packing arrangements of the cone  
10 photoreceptors.



12  
13 Figure 3. Grading scheme of retinal vasculature into sub-branches of progressively smaller caliber  
14

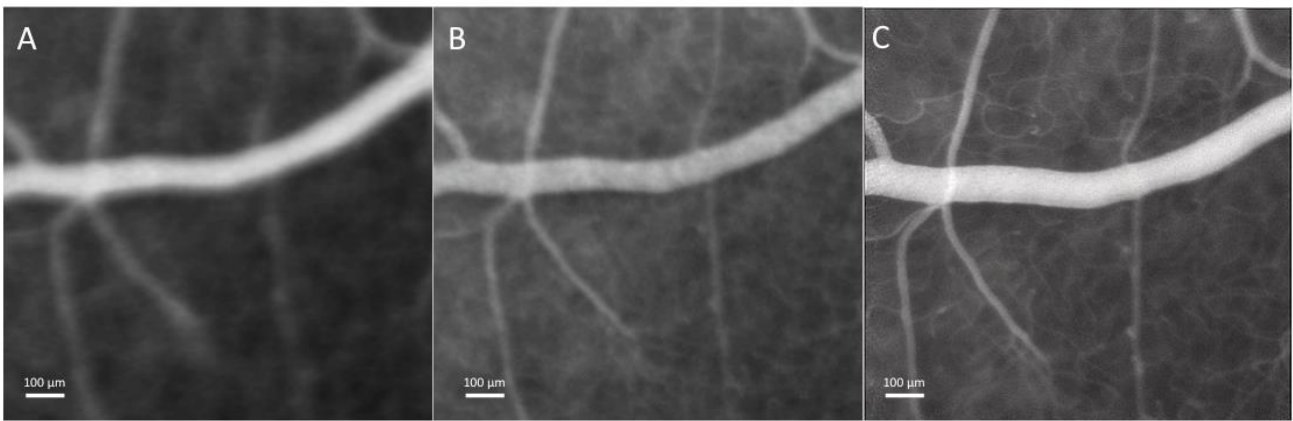
## 15 16 **Results**

17  
18 A total of 10 participants were enrolled in the study, with a mean age of 47.5 years  
19 (range 27 – 77) with half being male (n=5, 50%). The demographic features and  
20 diagnosis for each participant are listed in Table 1. All patients tolerated the imaging  
21 well.

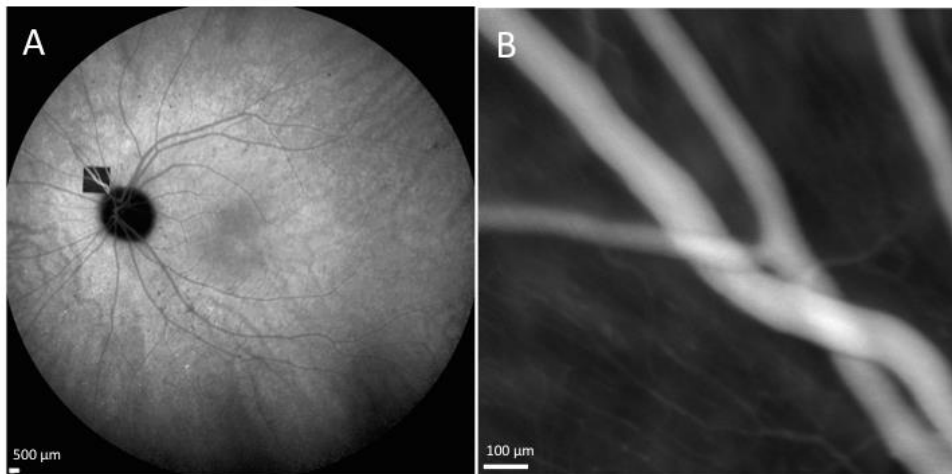
### 22 23 *High-resolution Fluorescein and Indocyanine Green Angiography*

24 In contrast to the standard images, the high-resolution images demonstrated greater  
25 visualization of smaller caliber vessels including its sub-branches (mean 1.2 greater  
26 sub-branches visible, median of 1 level, range 0-2) (Table 2). In the participant with

1 FFA performed on three different FA devices, the highest resolution, as determined  
2 by visibility of sub-branches, was seen in the modified HRA2 device, followed by the  
3 Topcon TRC-NW8 then the conventional HRA2 (Figure 4). Similarly, high resolution  
4 ICGA demonstrated visualization of smaller caliber branches with greater  
5 appreciation of the spatial relationship between vessels (Figure 5 and 6). Across all  
6 participants imaged using the high-resolution device however, there were variations in  
7 the clarity and fluorescence strength of the images obtained. In the first patient  
8 imaged, the HRA2 image was of poor quality and ungradable, likely due to delayed  
9 timing of the imaging. Earlier onset of angiography imaging immediately after dye  
10 injection produced better quality images of the capillary network, compared to when  
11 imaging was delayed by > 10 minutes.  
12



14 Figure 4. Comparison of enlarged conventional fundus fluorescein angiography (FFA) on Heidelberg retina  
15 angiography 2 (HRA) (A), Topcon TRC-NW8 (B) and high-resolution HRA2 (C) in the same location  
16



17  
18 Figure 5. Localization (A) and (B) early phase high-resolution indocyanine green angiography

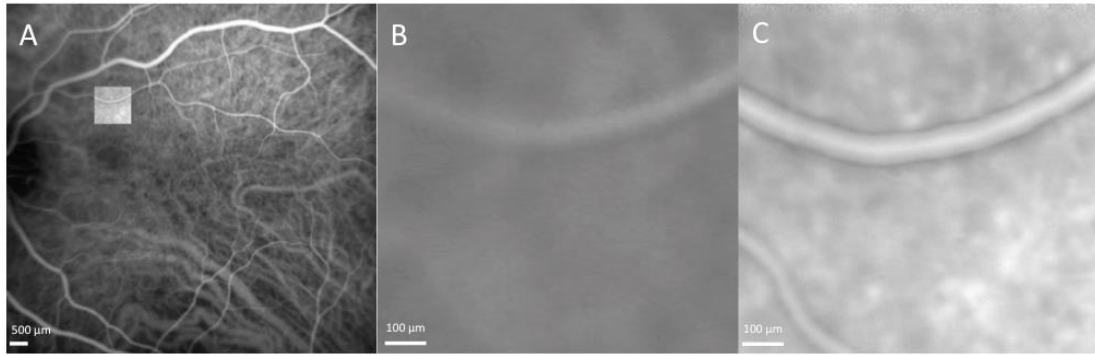
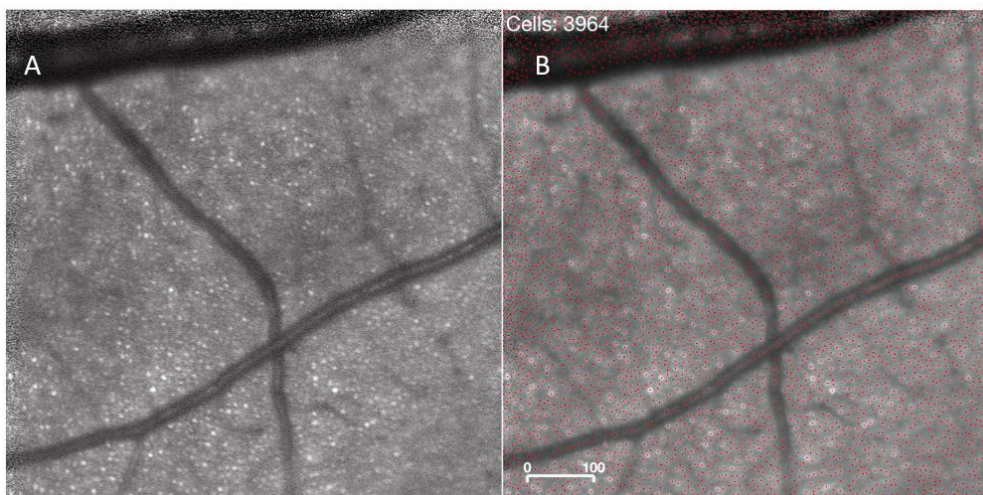


Figure 6. Localization and scaling of conventional indocyanine green angiography image (A) with enlarged conventional image (B) and high-resolution image (C)

Aside from capturing static images, the HRA2 can also be employed to take videos of the retinal vasculature in real time. No differences were seen on the videography setting when performing the high-resolution FFA or ICGA as compared to the static images. However, when the modified device was set to continuous infrared mode, flow of blood cells was discernible, visualized as continuous movement within the retinal circulation (supplementary material video file).

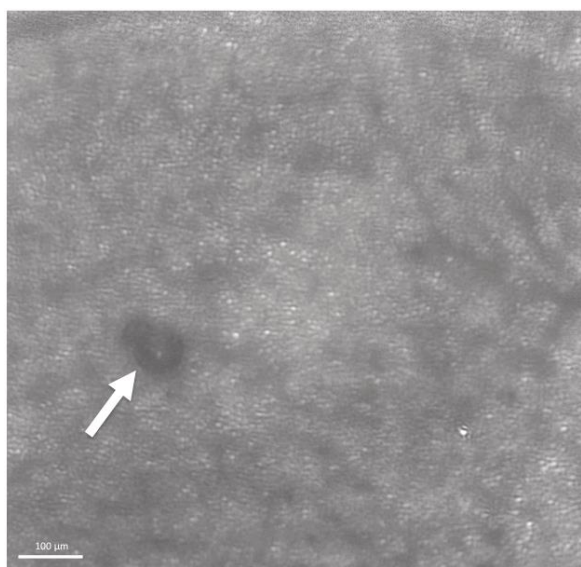
#### *Photoreceptor Mosaic Imaging and Analysis*

High-resolution images of the photoreceptor mosaic were also acquired using the infrared and blue reflectance setting. Imaging of the cone photoreceptors was resolved to a level sufficient for manual cone counting in both modalities (Figure 7, cone density 3964 cells/mm<sup>2</sup> including blood vessels, and 4695 cells/mm<sup>2</sup> accounting for blood vessels, hexagonal percentage 6273%, 39.6 μm spacing). Assessment of the photoreceptor density could also be obtained around microvascular structures of interest, such as a large microaneurysm in a diabetic patient (Figure 8, cone density 6397 cells/mm<sup>2</sup> without blood vessels, hexagonal percentage 10164%, 36.8 μm spacing). The device could be easily switched from infrared to angiography mode to provide an estimate of the cone density relative to perfusion in a given location (Figure 9, cone density 4846 cells/mm<sup>2</sup> without blood vessels, hexagonal percentage 6521%, 40.3 μm spacing).



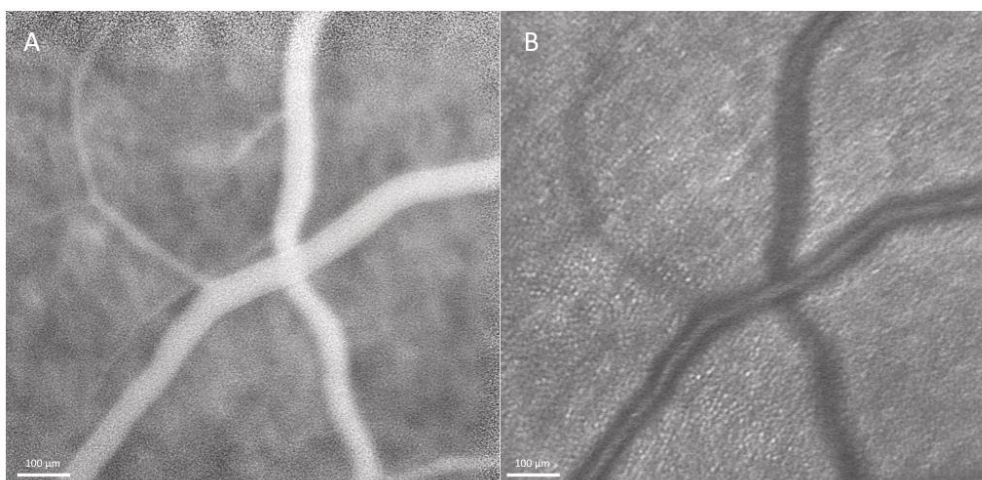
1  
2  
3  
4  
5

Figure 7. (A) High-resolution infrared image focused at the level of photoreceptor mosaic. (B) Automated assessment of cone density. Note few cones were detected within vessels and were manually excluded from the overall count (manual correction 4695 cells/mm<sup>2</sup>).



6  
7  
8  
9

Figure 8. High resolution infrared image of a patient with diabetic retinopathy demonstrating large microaneurysm (arrow) and adjacent photoreceptor mosaic (cone density 6397 cells/mm<sup>2</sup> excluding blood vessels)



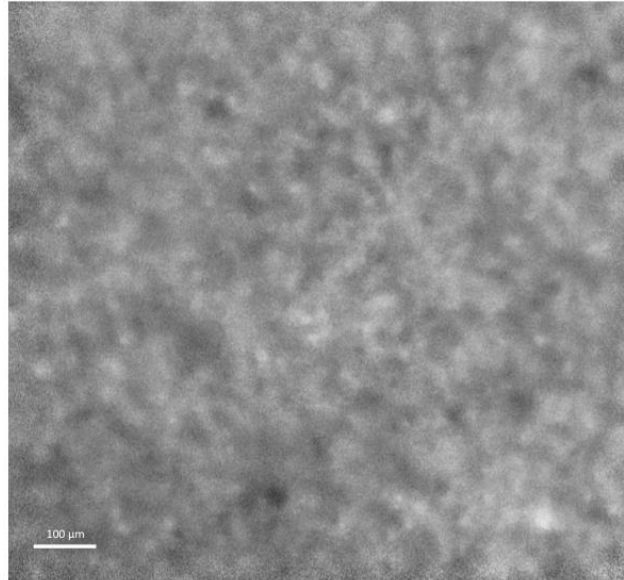
10  
11  
12

Figure 9. High-resolution fluorescein angiography images (A) and infrared imaging of photoreceptor mosaic (B) at the same location (cone density 4846 cells/mm<sup>2</sup> excluding blood vessels)

1  
2  
3  
4  
5

## *Imaging of Choriocapillaris*

In addition to standard angiography, the modified device also enabled imaging of the choriocapillaris layer by using the IRAF setting with ICG dye in situ. (Figure 10).



6  
7  
8  
9

Figure 10. Imaging of choriocapillaris layer with high-resolution indocyanine green angiography

## **Discussion**

11  
12  
13  
14  
15  
16  
17  
18  
19  
20  
21  
22

This is the first study to demonstrate that high-resolution *in vivo* fundus angiography is possible without the need for complex adaptive optics imaging systems. Fine retinal capillaries and its sub-branches were visualized with the narrow angle modification and there was improved spatial resolution of larger vessels on FFA and ICGA compared to conventional images. The system was also capable of demonstrating the topographic relationship between vessels and the photoreceptor mosaic on a single device, with cone density counts comparable to levels previously reported on AOSLO and on histology.<sup>13,14</sup> In addition, the videographic capabilities of the modified HRA2 system was also able to capture, movement of blood cells through the retinal circulation in real time.

23  
24  
25

Our results are comparable to those obtained using AOSLO FA. In a study by Pinhas et al., FFA was performed using confocal AOSLO in ten healthy subjects given oral or intravenous fluorescein dye.<sup>7</sup> Compared to conventional FFA, confocal AOSLO

1 FA demonstrated increased transverse and axial resolution and was able to resolve  
2 details of the retinal capillary bed and its sub-branches. Although we did not perform  
3 AOSLO FA in our subjects, retinal images acquired using the modified HRA2 device  
4 in this study had potential resolution down to the same capillary level as seen in the  
5 confocal AOSLO FA report.<sup>7</sup>

6

7 The ability to resolve fine retinal capillary details without the use of AO systems  
8 represents a significant advantage. Image acquisition using the high-resolution device  
9 is fast and can be viewed immediately without the need for complex image  
10 processing. In addition, the device is a modification of a conventional HRA2, a  
11 platform already familiar to many technicians, thus facilitating ease of use. It can also  
12 potentially be used to image a wider spectrum of patients including those with small  
13 pupils. However, both AOSLO FA and the modified HRA2 require oral or  
14 intravenous dye administration to view the retinal vasculature.

15

16 Optical coherence tomography angiography is another imaging modality that can  
17 provide high resolution images of the retinal vasculature. It does not require dye  
18 injection and as it is non-invasive, can be repeated at same or multiple visits with  
19 good reproducibility.<sup>15</sup> Although limited in its field of view, newer models in  
20 development are utilizing montaging protocols to allow wider field images of up to 70  
21 degrees.<sup>16,17</sup> Compared to traditional dye based angiography such as this however, its  
22 main disadvantage is its inability to demonstrate vascular leakage or areas of slow  
23 flow.

24

25 Limitations of this study include the small number of patients and the variation in the  
26 start time and fluorescence signal of the high-resolution FA due to the need to move  
27 patients from one device to another. In order to avoid subjecting patients to repeat  
28 angiograms, early phase images were only captured on one device at a time. A greater  
29 difference between the two devices may have been obtained if all the high-resolution  
30 imaging was performed in the early phase. There were also technical challenges in the  
31 reproducibility of the quality of the images. In addition, although the modified device  
32 provided improved visualization of smaller capillaries, the reduced field of view led  
33 to difficulties localizing where the image was being taken at the exact time of  
34 imaging. Montaging the images may help recreate a larger field of view; future  
35 modifications to the system to enable switching from the conventional to high-



1 resolution scanning angle within the same device would also be desirable to allow  
2 rapid examination of targeted features. However, as an exploratory study, the results  
3 of this study suggest the potential level of detail that can be obtained. Further studies,  
4 including early phase high-resolution FFA in all patients as compared with either  
5 OCTA or FA AOSLO, and dedicated imaging of pathology such as microaneurysms  
6 or neovascularization will help clarify the scope of this technology.

7

8 The study of microvascular abnormalities remains vital to understanding the  
9 pathobiology of retinal vascular diseases. Advances in imaging technology such as  
10 this, which allow detailed in vivo assessment of the vascular network simultaneously  
11 with the surrounding neuroretina, has the potential to identify earlier manifestations of  
12 a disease and improve our understanding of the relationship between photoreceptors  
13 and retinal vasculature. This is important, not only for diagnostic purposes, but may  
14 have a role in phenotyping patients for novel future therapies. In addition, the ability  
15 to assess photoreceptor density alongside vascular abnormalities can provide insight  
16 into the relationship between the two, an important factor in determining the timing of  
17 intervention needed for disease prevention. This high-resolution FA technology  
18 provides a promising avenue to better understand microvascular changes in both  
19 health and disease.

20

21

22

23

24

25

26

27

28

## 1   **References**

- 2   1. Novotny HR, Alvis DL. A method of photographing fluorescence in circulating  
3       blood in the human retina. *Circulation*. 1961;24. doi:10.1161/01.CIR.24.1.82
- 4   2. Gao SS, Jia Y, Zhang M, et al. Optical Coherence Tomography Angiography.  
5       *Invest Ophthalmol Vis Sci*. 2016;57(9):OCT27-OCT36. doi:10.1167/iovs.15-  
6       19043
- 7   3. Chui TYP, Mo S, Krawitz B, et al. Human retinal microvascular imaging using  
8       adaptive optics scanning light ophthalmoscopy. *Int J Retina Vitre*. 2016;2:11.  
9       doi:10.1186/s40942-016-0037-8
- 10  4. Roorda A, Romero-Borja F, Donnelly Iii W, Queener H, Hebert T, Campbell M.  
11       Adaptive optics scanning laser ophthalmoscopy. *Opt Express*. 2002;10(9):405-  
12       412.
- 13  5. Paques M, Meimon S, Rossant F, et al. Adaptive optics ophthalmoscopy:  
14       Application to age-related macular degeneration and vascular diseases. *Prog*  
15       *Retin Eye Res*. July 2018. doi:10.1016/j.preteyeres.2018.07.001
- 16  6. Chui TYP, Dubow M, Pinhas A, et al. Comparison of adaptive optics scanning  
17       light ophthalmoscopic fluorescein angiography and offset pinhole imaging.  
18       *Biomed Opt Express*. 2014;5(4):1173-1189. doi:10.1364/BOE.5.001173
- 19  7. Pinhas A, Dubow M, Shah N, et al. In vivo imaging of human retinal  
20       microvasculature using adaptive optics scanning light ophthalmoscope  
21       fluorescein angiography. *Biomed Opt Express*. 2013;4(8):1305-1317.  
22       doi:10.1364/BOE.4.001305
- 23  8. Dubow M, Pinhas A, Shah N, et al. Classification of human retinal  
24       microaneurysms using adaptive optics scanning light ophthalmoscope fluorescein  
25       angiography. *Invest Ophthalmol Vis Sci*. 2014;55(3):1299-1309.  
26       doi:10.1167/iovs.13-13122
- 27  9. Matlach J, Mulholland PJ, Cilkova M, et al. Relationship between Psychophysical  
28       Measures of Retinal Ganglion Cell Density and In Vivo Measures of Cone  
29       Density in Glaucoma. *Ophthalmology*. 2017;124(3):310-319.  
30       doi:10.1016/j.opthta.2016.10.029
- 31  10. Wolsley CJ, Saunders KJ, Silvestri G, Anderson RS. Comparing mfERGs with  
32       estimates of cone density from in vivo imaging of the photoreceptor mosaic using  
33       a modified Heidelberg retina tomograph. *Vision Res*. 2010;50(15):1462-1468.  
34       doi:10.1016/j.visres.2010.04.015
- 35  11. Drasdo N, Fowler CW. Non-linear projection of the retinal image in a wide-angle  
36       schematic eye. *Br J Ophthalmol*. 1974;58(8):709-714.
- 37  12. Li KY, Roorda A. Automated identification of cone photoreceptors in adaptive  
38       optics retinal images. *J Opt Soc Am A Opt Image Sci Vis*. 2007;24(5):1358-1363.
- 39  13. Park SP, Chung JK, Greenstein V, Tsang SH, Chang S. A study of factors  
40       affecting the human cone photoreceptor density measured by adaptive optics



- 1 scanning laser ophthalmoscope. *Exp Eye Res.* 2013;108:1-9.  
2 doi:10.1016/j.exer.2012.12.011
- 3 14. Jonas JB, Schneider U, Naumann GO. Count and density of human retinal  
4 photoreceptors. *Graefes Arch Clin Exp Ophthalmol Albrecht Von Graefes Arch*  
5 *Klin Exp Ophthalmol.* 1992;230(6):505-510.
- 6 15. Spaide RF, Fujimoto JG, Waheed NK, Sadda SR, Staurengi G. Optical  
7 coherence tomography angiography. *Prog Retin Eye Res.* 2018;64:1-55.  
8 doi:10.1016/j.preteyeres.2017.11.003
- 9 16. Hirano T, Kakihara S, Toriyama Y, Nittala MG, Murata T, Sadda S. Wide-field  
10 en face swept-source optical coherence tomography angiography using extended  
11 field imaging in diabetic retinopathy. *Br J Ophthalmol.* 2018;102(9):1199-1203.  
12 doi:10.1136/bjophthalmol-2017-311358
- 13 17. Zhang Q, Rezaei KA, Saraf SS, Chu Z, Wang F, Wang RK. Ultra-wide optical  
14 coherence tomography angiography in diabetic retinopathy. *Quant Imaging Med*  
15 *Surg.* 2018;8(8):743-753. doi:10.21037/qims.2018.09.02
- 16  
17

1 **Tables**

2

3 Table 1. Clinical characteristics of participants

4

5 Table 2. Comparison of retinal vascular tree sub-branches visible between  
6 conventional and high-resolution fundus angiography

7

8

Table 1. Clinical characteristics of participants

| Participant | Age (years) | Gender | Right BCVA (Snellen) | Left BCVA (Snellen) | Diagnosis                          |
|-------------|-------------|--------|----------------------|---------------------|------------------------------------|
| 1           | 68          | F      | 6/6                  | 6/7.5               | Macular telangiectasia type 2      |
| 2           | 36          | M      | 6/4                  | 6/4                 | Central serous chorioretinopathy   |
| 3           | 58          | M      | 6/9.5                | 6/8                 | Age related macular degeneration   |
| 4           | 52          | F      | 6/5                  | 6/6                 | Macular telangiectasia type 2      |
| 5           | 56          | F      | 6/5                  | 6/5                 | Proliferative diabetic retinopathy |
| 6           | 38          | M      | 6/5                  | 6/12                | Central serous chorioretinopathy   |
| 7           | 77          | F      | 6/7.5                | 6/9                 | Macular telangiectasia type 2      |
| 8           | 30          | F      | 6/6                  | 6/6                 | Healthy control                    |
| 9           | 33          | M      | 6/6                  | 6.6                 | Healthy control                    |
| 10          | 27          | M      | 6/6                  | 6/6                 | Healthy control                    |

F = Female; M = Male; BCVA = best-corrected visual acuity

Table 2. Comparison of retinal vascular tree sub-branches visible between conventional and high-resolution fundus angiography

| Participant | Conventional Image | High-resolution Image | Difference   |
|-------------|--------------------|-----------------------|--------------|
| 1           | 2                  | Poor quality          | Not gradable |
| 2           | 2                  | 2                     | 0            |
| 3           | 2                  | 3                     | +1           |
| 4           | 3                  | 4                     | +1           |
| 5           | 1                  | 2                     | +2           |
| 6           | 2                  | 4                     | +2           |
| 7           | 2                  | 2                     | 0            |
| 8           | 2                  | 4                     | +2           |
| 9           | 2                  | 4                     | +2           |
| 10          | 3                  | 4                     | +1           |